11-15-2010

[Fe-Fe]-Hydrogenase Reactivated by Residue Mutations as Bridging Carbonyl Rearranges: A QM/MM Study

Stefan Motiu
Cleveland State University

Valentin Gogonea
Cleveland State University, v.gogonea@gmail.com

[Fe-Fe]-Hydrogenase Reactivated by Residue Mutations as Bridging Carbonyl Rearranges: A QM/MM Study

STEFAN MOTIU, VALENTIN GOGONEA

Introduction

[Fe-Fe]- and [Ni-Fe]-hydrogenases are two major classes of enzymes that reversibly catalyze the apparently simple reaction of protons and electrons to molecular hydrogen, $2H^+ + 2e^- \leftrightarrows H_2$, which occurs in anaerobic media. In living systems, of the two metalloproteins, [Fe-Fe]-hydrogenases are mostly used for H_2 production, having a reactivity of about 2 orders of magnitude larger than [Ni-Fe]-hydrogenases. These enzymes are found in many bacteria, simple eukaryotes, and archaea where they provide H_2 for the metabolic processes of these life forms. By means of H_2 oxidation, ATP synthesis exploits H_2 as an energy source, whereas H_2 synthesis results from the metabolic disposal of excess electron (with available H^+s), or from pyruvate fermentation. Proteins, such as ferredoxins, cytochrome C3, and cytochrome C6, act as physiological e^- donors or acceptors [1–3]. The exploration of alternative energy sources has kindled great interest in hydrogenase research. The reason for studying biological H_2 production is to clarify the complex mechanism (for hydrogen synthesis), which may help researchers produce clean fuel [4], using certain anaerobic organisms [5–8].

This theoretical study aims to find ways of making these enzymes function aerobically (to provide clean fuel, viz., H_2[1]), because they become inactivated by exogenous ligands such as O_2, OH^-, and H_2O [9, 10]. Water is the metabolic product of the inactivated catalytic site, that is, $(Fe_d-)OO \rightarrow (Fe_d-)H_2O$[1], and it also binds to the hydrogenase active site in its resting state, viz., $Fe^{II}Fe^{II}$ [11, 12].

By performing Density Functional Theory (DFT) calculations on the H-cluster, with H_2O, OH^-, and O_2 bound to Fe_d, (redox states Fe^{II}-Fe^{I}), Liu and Hu [10] have inferred, based on agreement between calculated and experimental vibrational frequencies of the three endogenous CO ligands, that OH^- is the oxygen species which inhibits hydrogenases. The X-ray structures of [Fe-Fe]-hydrogenases, from *Clostridium pasteurianum* (CPI)[11] and *Desulfovibrio desulfuricans* (DdH),[13] can be used to theoretically investigate their functions via biochemical pathways [10, 14]. Since former DFT and hybrid quantum mechanics/molecular mechanics (QM/MM), calculations [9, 10, 14, 15, 16–22] have shown success in clarifying certain aspects of the catalytic properties of the H-cluster; similar methodologies are also used in our investigation. In our study, as well as in other computational studies [9, 10, 14, 15, 19, 20], CH_3-S^- has been substituted for cysteine, Cys^{382}, and H^+ for the proximal cubane.[2]

The active site of hydrogenases, viz., the H-cluster (see Fig. 1), is comprised of a dimetal complex, [Fe-Fe], with the metal centers being bridged by di(thiomethyl)amine (DTMA), and a cubane subunit, $[Fe_4$-$S_4]^{2+}$. The iron atoms are coordinated by endogenous ligands, viz., two cyanides (CN^-), two terminal carbonyls (CO_t), and a bridging carbonyl (CO_b).[3] An Fe atom, which is part of the proximal

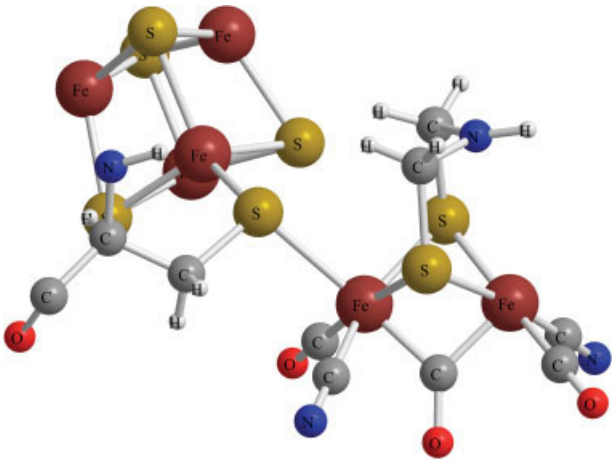

FIGURE 1. The H-cluster structure. [Color figure can be viewed in the online issue, which is available at wileyonlinelibrary.com.]

cubane subunit, $[Fe_4\text{-}S_4]^{2+}{}_p$, is linked to the Fe_p of the di-iron subunit, $[Fe_p\text{-}Fe_d]$, through a cysteinyl sulfur (or S_γ of Cys^{382}).

In spite of the di-iron H-cluster subunit redox states, the proximal cubane remains in oxidation [23] state II, $[Fe_4\text{-}S_4]^{2+}{}_p$. Computational and experimental [Fe-Fe]-hydrogenase H-cluster (and synthetic H-cluster analogues) research [3, 4, 9, 10, 12–15, 19, 21, 24–52] corroborates the potential redox states of the di-iron H-cluster subunit, $Fe_p\text{-}Fe_d$, where $Fe_p{}^{I}\text{-}Fe_d{}^{I}$, EPR silent, is the reduced di-iron H-cluster subunit, $Fe_p{}^{II}\text{-}Fe_d{}^{I}$, paramagnetic, is the partially oxidized, and catalytically active di-iron subunit, and $Fe_p{}^{II}\text{-}Fe_d{}^{II}$, EPR silent [13, 53], is the fully oxidized, inactive biferrous subunit, and has an OH^- or H_2O molecule bound to the $Fe_d{}^{II}$.

By performing spectroscopic studies on [Fe-Fe]-hydrogenases, which have been purified from *Clostridium pasteurianum* and *Desulfovibrio desulfuricans*, their catalytic functions have been elucidated [11–13, 54, 55]. An X-ray crystal structure of CPI hydrogenase shows an (inactivating) oxygen species that may be OH^- or H_2O bound to the Fe_d of the H-cluster, while the other X-ray structure has an inactivating CO bound to Fe_d [11, 12]. For this study, DdH has been selected because its crystal structure has a better resolution (viz., 1.6 Å), than CPI (viz, 1.8 Å) [11, 13].

This investigation is subdivided into three parts, viz., thermodynamics, geometric, and electronic analysis, for both wild-type and mutated (residue substituted) DdH. These analyses were carried out in order to understand the thermodynamic results, their relationship to certain molecular spatial behavior, for example, CO_b movement, and the electronic structural methods, such as frontier molecular orbitals (FMO) and natural bond orbital partial charges (NBO).

Methods

The ONIOM method [56] (DFT for the QM region, and the universal force field, UFF [57], for the MM region, implemented in Gaussian03 [58]) has been utilized to determine the reaction thermodynamics, viz., ΔG for individual reaction steps, of the [Fe-Fe]-hydrogenase H-cluster (the active group of DdH) reactivation.

Low spin states (singlet and doublet) and low oxidation states (I and II) have been used for the di-irons [10, 19] in agreement with the experimental and computational data.

The electronic structure of the hydrogenase H-cluster (without proximal cubane) has been determined using DFT method (B3LYP functional [59, 60]), and 6–31+G(d,p) basis set.

Hydrogen atoms were added to the X-ray crystal structure of DdH using the Gromacs program [61, 62] [Brookhaven Protein Data Bank id.1HFE]. After the structure has been solvated [2,043 H_2O molecules (in 1 nm layer peripheral to H-cluster)], six Na^+ ions were randomly incorporated into the solvent (7 Na^+ ions for clusters 1, 3, 4; 8 Na^+ ions for cluster 2) to neutralize the negative charges [23] on the H-cluster, medial, and distal cubane/cysteines clusters.[4] At physiological pH (~7), Gromacs program considers negative charges on the acidic residues (28 Asp and 33 Glu), and positive charges on the most basic residues (44 Lys and 15 Arg).

Out of the 13 His found in DdH, only two are protonated, and these charges (in conjunction with those from Lys and Arg) are used to neutralize the negatively charged residues, viz., Asp and Glu. Thus, the overall apoprotein charge is zero, except the 12 negatively charged cysteines bound to the iron atoms of the three cubanes, where each has a charge of 2+.

Geometry optimizations have been performed in aqueous enzyme phase, where residues in the MM region (except the proximal cubane), and Fe_p and

$CO_{t,p}$, in the QM region have been kept frozen.[5] The rational for freezing Fe_p and $CO_{t,p}$ arises from former optimizations [15] where they were found to spatially rearrange the least. Once geometry optimizations have been carried out for DdH, frequency calculations are performed in order to obtain thermodynamic data, viz., ΔG. Frequency calculations treat both the apoenzyme and the cubanes as partial charges, whereas [Fe_p-Fe_d] subunit is treated at DFT level.

The DdH apoenzyme and cubanes, viz., proximal, medial, and distal are included in the MM region. The QM region consists of the [Fe_p-Fe_d] subunit (the moiety of H-cluster), and C_β and S_γ (cysteinyl sulfur of Cys^{382}). To avoid dangling bonds between the ONIOM layers, two linking hydrogen atoms were added between S_γ and Fe (of the proximal cubane), and between C_α and C_β (of Cys^{382}).

The UFF charge equilibration method was utilized to describe the electrostatic interactions within the MM region of DdH, whereas the solvent charges ($q_O = -0.706$ a.u. and $q_H = 0.353$ a.u.) were obtained from literature [30].

Then, a DdH sphere with a radius of 8 Å from Fe_d was investigated regarding the potential inhibitory residues for H_2O removal. H-cluster hindering residues (for H_2O elimination) are identified by using QM/MM geometry optimizations, and then their influence on thermodynamics and electronic properties of the catalytic site is assessed. Given that water is polar, candidate, potential inhibitory residues should also be polar. Then, potential, polar inhibitory residues are screened to identify the most probable residues that hinder H_2O from leaving the catalytic site. Screening is the process whereby polar residues are removed (from within a sphere of radius 8 Å), one at a time, which is followed by frequency calculations aiming to learn whether the binding energy of water has decreased. If successful, then further residue substitutions are performed, that is, a neutral polar residue is substituted for a neutral, nonpolar residue, and an acidic residue is substituted for a basic residue, and vice versa.[6] Then, after each substitution, geometry optimization is performed, followed by frequency calculations to obtain the Gibbs' energy of H_2O dissociation.

Lastly, Gibbs' energies of H_2O and H_3O^+ (viz., $\Delta G_{H2O} = -76.419750$, and $\Delta G_{H3O}{}^+ = -76.598767$ Hartrees/molecule), which are needed for thermodynamic analysis, have been obtained by performing frequency calculations on these molecules which were positioned in the H-cluster cavity surrounded by the apoenzyme and the cubanes.

[5]A "frozen" enzyme method, (used for hybrid QM/MM setup) has its Cartesian coordinates of the selected atoms kept "fixed" in space, has advantages in acquiring results, and lessens the computational time.

[6]The Pymol program [63] has been used to measure interatomic distances between oxygen (of the exogenous H_2O) and terminal atoms (excluding hydrogens) of residue R-groups; it was also used for residue substitutions. The Swiss PDB Viewer [64] was utilized to add H^+s to obtain protonated histidines.

Results

THERMODYNAMIC ANALYSIS

The reactivation mechanism of [Fe-Fe]-hydrogenase H-cluster essentially consists of three reaction steps, viz., protonation, reduction, and H_2O elimination. The reactivation pathways (Schemes 1–3) proceed with different combinations for the three steps.

For the hybrid calculations, the reductive step, 1 → 2 (Scheme 1), of [Fe^{II}-Fe^{II}]-hydrogenase H-cluster proceeds rather endergonically, viz., $\Delta G_{Enzyme} = +42.6$ kcal/mol (Table I) relative to the gas phase ($\Delta G_{Gas\ \Phi} = +8.2$ kcal/mol, Table I), which points out that DdH reduction is less spontaneous than in vacuum, emphasizing the stereoelectronic effects of the apoenzyme, the medial, and distal cubanes on the H-cluster. The protonation step, 2 → 3 (Scheme 1), is highly exergonic ($\Delta G_{Enzyme\ \Phi} = -317.9$ kcal/mol, see Supporting Information Table I for protonation free energies using an alternative protonation source). The Gibbs' energy difference between the reactions of the two environments (i.e., vacuum vs. enzyme Φ, Table I) is +91.3 kcal/mol, and points to a more spontaneous reaction in gas phase. In step 3 → 4 (H_2O elimination), the hydrogenase H-cluster calculations show a rather small, endergonic result ($\Delta G_{Enzyme\ \Phi} = +2.0$ kcal/mol), as opposed to the exergonic gas phase outcome ($\Delta G_{Gas\ \Phi} = -6.6$ kcal/mol). The enzymatic H_2O removal is nonspontaneous due to the influence of the protein environment on the H-cluster electronic properties.

The DdH protonation, 1 → 2′ (Scheme 2), provides an exergonic reaction, viz., $\Delta G_{Enzyme\ \Phi} = -236.8$ kcal/mol, proceeding less spontaneously than in gas phase, viz. $\Delta G_{Gas\ \Phi} = -328.3$ kcal/mol, correlating the trend in Scheme 1. The enzyme Φ calculations, for the H_2O removal, 2′ → 3′, (Scheme 2), confer an endergonic result, ($\Delta G_{Enzyme\ \Phi} = +22.9$ kcal/mol), as opposed to the exergonic gas Φ

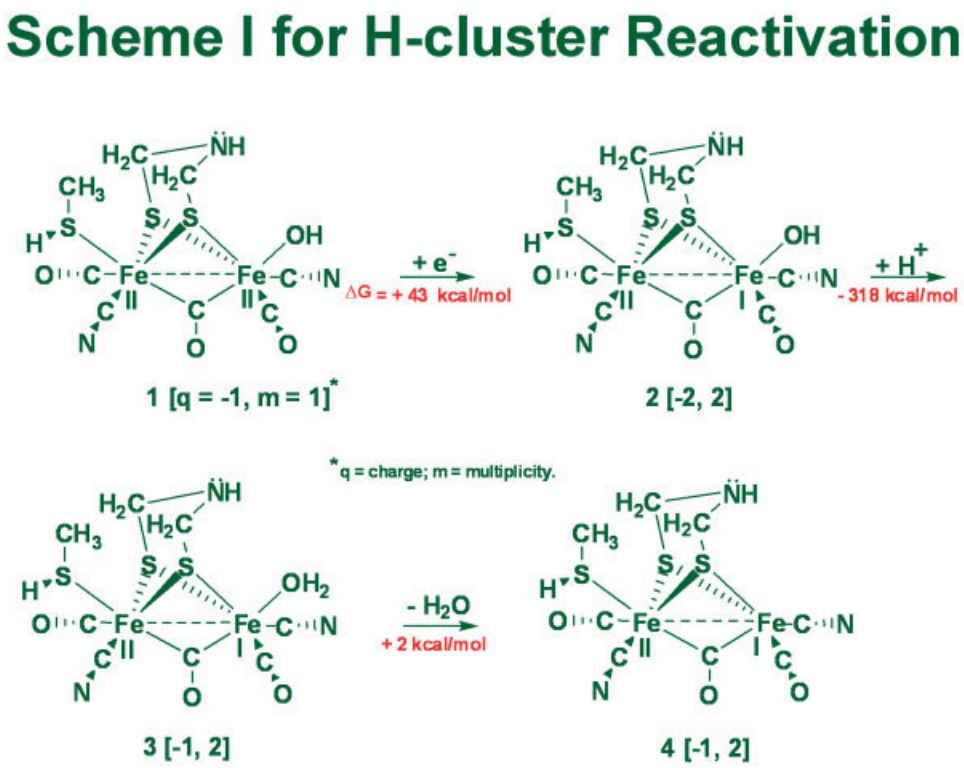

SCHEME 1. The reactivation pathway I of [Fe-Fe]-hydrogenase H-cluster. [Color figure can be viewed in the online issue, which is available at wileyonlinelibrary.com.]

reaction step ($\Delta G_{\text{Gas }\Phi} = -16.6$ kcal/mol), which results in a difference of +39.5 kcal/mol. Again, the effect of the protein environment is manifest on the individual steps of the reaction mechanism. The final reductive step, 3′ → 4, of the aqueous enzyme Φ (Scheme 2) proceeds exergonically, viz., $\Delta G_{\text{Enzyme }\Phi} = -59.4$ kcal/mol, close to the gas phase result, viz., $\Delta G_{\text{Gas }\Phi} = -62.7$ kcal/mol.

However, Scheme 3, in contrast, definitely provides room for enhancements that could achieve H_2O removal because, in step 3 → 4, the hydrogenase H-cluster calculations provide a rather small, free energy, viz., $\Delta G_{\text{Enzyme }\Phi} = +2.0$ kcal/mol, which could be changed into an exergonic reaction via mutagenesis. For Scheme 3, only the H_2O removal step is endergonic (viz., $\Delta G_{\text{Enzyme }\Phi} = +2.0$ kcal/mol, as in Scheme 1), whereas the other remaining steps [protonation (viz., $\Delta G_{\text{Enzyme }\Phi} = -236.8$ kcal/mol), reduction (viz., $\Delta G_{\text{Enzyme }\Phi} = -38.4$ kcal/mol)] are exergonic.

The following investigation addresses possible reactivation mechanisms of DdH mutants, uses the QM/MM method for pathway I, II, and III, and aims for the removal of H_2O.

The wild-type hydrogenase has been residue manipulated in two ways. First of all, the considered residues (Table I) have been removed one at a time in order to find which are responsible for keeping the water from being displaced. Subsequently, for the six culprit residues, that proved to hinder the removal of water, substitutions had been carried out (as describe in the Methods section), viz., $Arg^{111}Glu$, $Thr^{145}Val$, $Ser^{177}Ala$, $Glu^{240}His$, $Glu^{374}His$, and $Tyr^{375}Phe$.

In Scheme 1, the reduction step, 1 → 2, upon the removal of Glu^{240}, becomes less endergonic by $\Delta G = +17.0$ kcal/mol (relative to wild-type DdH) but not even close to make it spontaneous.[7] For 2 → 3, with the removal of a basic residue, that is, Lys^{237} (when compared with the wild-type enzyme), the protonation step proceeds more exergonically, viz., by a Gibbs' energy difference of +27.3 kcal/mol. The last step, 3 → 4, proceeds exergonically, viz., $\Delta G_{\text{Enzyme }\Phi} = -1.6$ kcal/mol, upon the removal of Glu^{374} from the apoenzyme; however, Scheme 1

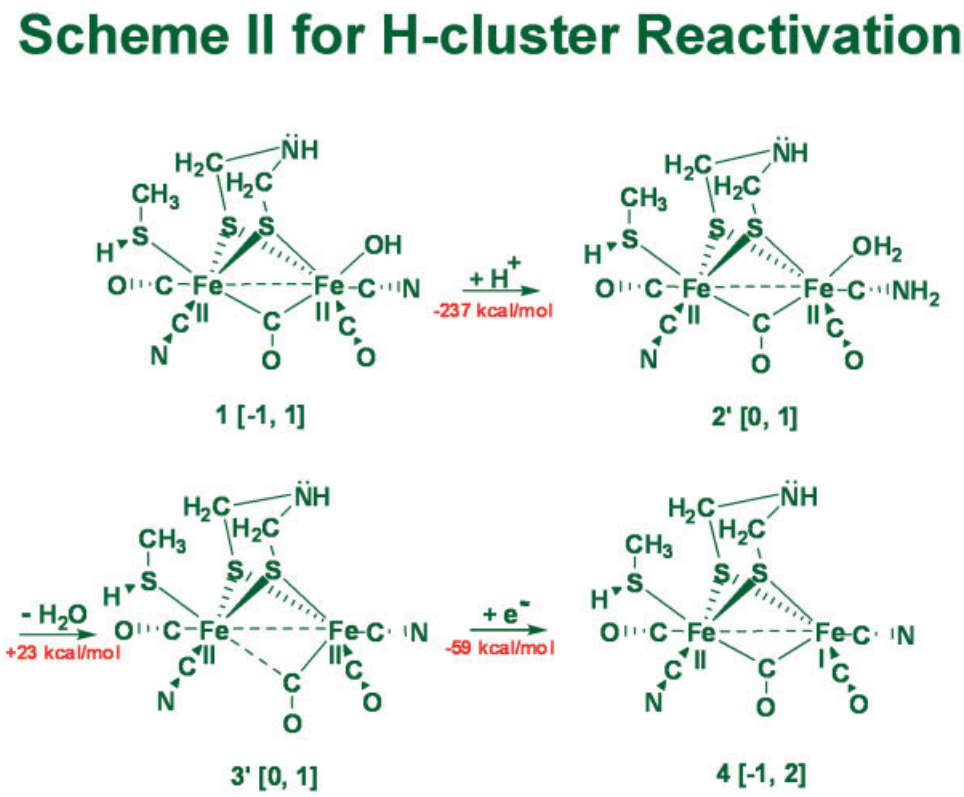

SCHEME 2. The reactivation pathway II of [Fe-Fe]-hydrogenase H-cluster. [Color figure can be viewed in the online issue, which is available at wileyonlinelibrary.com.]

cannot proceed to the completion due to the endergonic, reductive step, 1 → 2.

For Scheme 2, an improvement has been obtained (as in Scheme 1) upon the removal of exactly the same residue for each of the corresponding step, that is, Lys^{237} for protonation (viz., $\Delta G_{\text{Enzyme }\Phi} = -264.4$ kcal/mol), Glu^{240} for reduction (viz., $\Delta G_{\text{Enzyme }\Phi} = -78.7$ kcal/mol), and Glu^{374} for H_2O elimination (viz., $\Delta G_{\text{Enzyme }\Phi} = +21.5$ kcal/mol). However, in spite of Gibbs' energy improvements for all reaction steps, no matter what residues (Table I) are removed, Scheme 2 is hindered from completion in the H_2O removal step.

In Scheme 3, the only endergonic step is for the removal of H_2O ($\Delta G = +2.0$ kcal/mol), which was, nevertheless, made to proceed exergonically by eliminating several residues, one at a time. The most promising residues are ΔArg^{111}, ΔThr^{145}, ΔSer^{177}, ΔGlu^{240}, ΔGlu^{374}, and ΔTyr^{375}, and their respective deletion Gibbs' energies are −0.7 kcal/mol, −0.2 kcal/mol, −0.5 kcal/mol, +0.8 kcal/mol, −1.6 kcal/mol, and +1.1 kcal/mol (Table I). In 3 → 4, single residue substitutions have been carried out on the six residues that hinder the removal of water, viz., Arg^{111}Glu, Thr^{145}Val, Ser^{177}Ala, Glu^{240}His, Glu^{374}His, and Tyr^{375}Phe, followed by (sequential) frequency calculations.

Then out of the most successful substitutions, two, three, and four residue combinations were examined by frequency calculations (Table II). The 1st two-residue combination is Glu^{374}His and Tyr^{375}Phe giving $\Delta G = -5.1$ kcal/mol; the 2nd three-residue combination is Thr^{145}Val, Glu^{374}His, and Tyr^{375}Phe giving $\Delta G = -6.2$ kcal/mol, and the 3rd four-residue combination is Arg^{111}Glu, Thr^{145}Val, Glu^{374}His, and Tyr^{375}Phe giving $\Delta G = -7.5$ kcal/mol.

GEOMETRIC CONSIDERATIONS

To explain Gibbs' energies between the aqueous enzyme Φ and the gas Φ calculations, DdH H-cluster and H-cluster geometries for the two phases are analyzed, and then the hydrogenase H-cluster

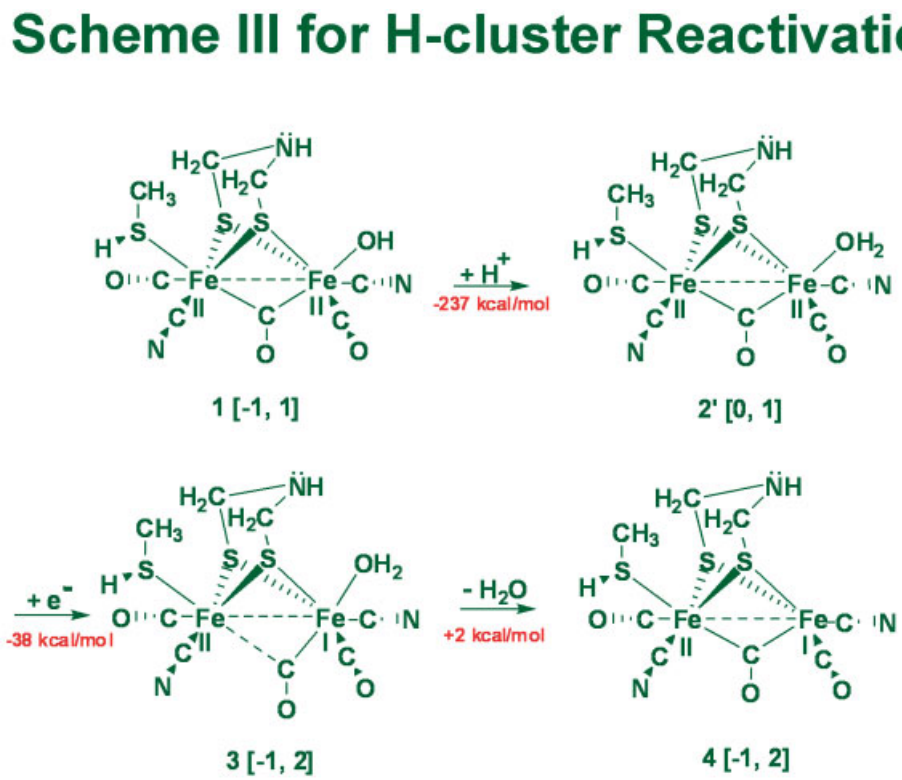

SCHEME 3. The reactivation pathway III of [Fe-Fe]-hydrogenase H-cluster. [Color figure can be viewed in the online issue, which is available at wileyonlinelibrary.com.]

distances to the six replaced, juxtaposed residues are presented for the aqueous enzyme Φ.

The wild-type DdH QM/MM calculations for H_2O removal, (3 → 4), reveal a contrasting picture regarding CO_b translation towards Fe_d relative to the gas phase H_2O elimination. That is, in Table III,[8] 3 → 4, the iron-carbon distance, Fe_d-CO_b, essentially remains constant [(viz., 1.907 Å → 1.908 Å), whereas the gas Φ distance becomes smaller (viz., 1.945 Å → 1.850 Å), and the reaction (3 → 4) is exergonic], [14, 15] which may explain why H_2O removal is endergonic for the enzyme Φ.

Thus, it is ascertained that for the aqueous enzyme Φ, an endergonic ligand (H_2O) dissociation is manifested in the Fe_p-CO_b bond contraction (1.959 Å → 1.939 Å). The opposite trend is observed in gas phase, where the Fe_p-CO_b bond is elongated (2.013 Å → 2.232 Å) after H_2O elimination.

Out of the three reaction pathways presented here, only Scheme 3 is analyzed for geometrical considerations, for it is the only one having the potential for metabolic reactivation by means of residue substitutions. The latter scheme has only the water removal step to be overcome in order to proceed exergonically, while, on the other hand, the other schemes cannot be made exergonic by residue substitutions.

Next, an analysis is provided for the interatomic distances (Å), between Fe_p and Fe_d, Fe_p and CO_b, Fe_d and CO_b, and Fe_d and H_2O, before and after water removal, to compare the H_2O elimination Gibbs' energies for the residue substituted DdH with the thermodynamics of the wild-type DdH.

For the removal of water from the wild-type enzyme, the distance between Fe_d and CO_b is slightly increasing (Table III), which corresponds to the endergonic step, viz., $\Delta G_{\text{Enzyme }\Phi} = +2.0$ kcal/mol. However, the H_2O removal from the mutated enzyme is exergonic (Table II), correlating to the movement of the CO_b towards the Fe_d. As a result of mutating DdH, the following bond contractions, Fe_d-CO_b, have been obtained, viz., 0.024 Å for $Arg^{111}Glu$, 0.028 Å for

TABLE I

Native and residue removed DdH Gibbs' energies (kcal/mol) for reaction steps of reactivation pathways I, II, and III.

Reaction steps	$(+e^-)$ $1 \rightarrow 2$	$(+H^+)$ $2 \rightarrow 3$	$(-H_2O)$ $3 \rightarrow 4$	$(+H^+)$ $1 \rightarrow 2'$	$(-H_2O)$ $2' \rightarrow 3'$	$(+e^-)$ $3' \rightarrow 4$	$(+e^-)$ $2' \rightarrow 3$
Native DdH	+42.6	−317.9	+2.0	−236.8	+22.9	−59.4	−38.4
$\Delta Ser^{62}s$[a]	+38.3	−313.6	+2.0	−232.6	+23.1	−63.9	−42.7
ΔArg^{111}	+59.0	−332.4	−0.7	−251.4	+22.0	−44.7	−22.0
ΔTyr^{112}	+47.5	−322.1	+1.6	−241.1	+22.8	−54.8	−33.6
ΔAsp^{144}	+28.8	−305.0	+3.0	−223.4	+24.1	−73.8	−52.8
ΔThr^{145}	+44.1	−318.8	−0.2	−237.9	+22.8	−59.9	−36.9
ΔGlu^{146}	+32.5	−308.5	+2.5	−227.4	+23.6	−69.7	−48.6
ΔThr^{148}	+41.8	−316.8	+1.8	−235.8	+22.9	−60.3	−39.2
ΔAsp^{150}	+32.8	−308.1	+2.1	−227.0	+23.3	−69.5	−48.3
ΔThr^{152}	+47.1	−322.6	+1.9	−241.6	+23.0	−55.1	−33.9
ΔGlu^{155}	+36.5	−311.4	+1.9	−230.2	+23.0	−65.8	−44.7
ΔThr^{176}	+43.8	−319.5	+2.1	−238.3	+23.2	−58.5	−37.4
ΔSer^{177}	+38.3	−312.8	−0.5	−231.8	+22.9	−66.1	−42.7
ΔGln^{183}	+46.3	−322.3	+2.3	−241.1	+23.3	−55.9	−34.9
ΔSer^{198}	+42.6	−318.0	+2.1	−236.9	+23.2	−59.6	−38.5
ΔLys^{201}	+48.3	−323.5	+1.7	−242.6	+22.7	−53.6	−32.6
ΔSer^{202}	+46.3	−324.1	+2.4	−241.8	+22.5	−56.0	−35.9
ΔAsn^{207}	+46.7	−321.6	+1.5	−240.6	+22.5	−55.2	−34.2
ΔSer^{230}	+38.2	−314.0	+2.3	−232.9	+23.3	−64.0	−42.9
ΔLys^{237}	+69.2	−345.2	+1.2	−264.4	+21.7	−32.1	−11.6
ΔLys^{238}	+47.4	−322.1	+1.7	−241.5	+22.9	−54.4	−33.3
ΔGlu^{240}	+25.6	−300.1	+0.8	−218.9	+23.8	−78.7	−55.6
ΔThr^{257}	+42.8	−318.0	+1.9	−236.9	+23.1	−59.5	−38.3
ΔThr^{259}	+45.9	−320.8	+1.8	−239.9	+23.0	−56.1	−35.0
ΔThr^{260}	+42.1	−317.4	+2.0	−236.4	+23.1	−60.1	−39.0
ΔSer^{289}	+44.0	−319.1	+1.9	−238.1	+22.9	−58.1	−37.0
ΔThr^{294}	+40.4	−316.0	+2.2	−234.9	+23.2	−61.8	−40.8
ΔThr^{299}	+40.9	−316.2	+1.9	−235.1	+23.0	−61.2	−40.1
ΔGlu^{374}	+27.7	−301.3	−1.6	−220.2	+21.5	−76.5	−53.4
ΔTyr^{375}	+41.5	−315.8	+1.1	−234.8	+22.3	−60.6	−39.5
ΔGln^{388}	+44.0	−319.2	+2.0	−238.1	+23.1	−58.2	−37.1
Gas ϕ	+8.2	−409.2	−6.6	−328.3	−16.6	−62.7	−72.7

[a] Residue removed DdH.

s = small chain.

$Thr^{145}Val$, 0.017 Å for $Glu^{374}His$, and 0.031 Å for $Tyr^{375}Phe$, corresponding to exergonic steps for water elimination (Table II).

Note that a simultaneous bond elongation occurs [for all presented mutations (Table III)] between the Fe_p and the bridging carbonyl, Fe_p-CO_b, when bond contraction for Fe_d-CO_b takes place. As a result of mutating DdH (vs. the wild-type enzyme), larger bond contractions between the iron atoms, Fe_d-Fe_p, have been obtained (ca. 0.1 Å, Table III). It is also noticed that the bond length between the distal iron and water, Fe_d-H_2O, is longer, that is, about 2.2 Å (vs. 2.1 Å) in the mutated DdH vs. the wild-type enzyme.

The following trend has been observed for some of the DdH mutants that the closer the substituted residue is to the H-cluster exogenous water (Table IV), the more spontaneous is the water removal step becomes. The exception is $Tyr^{375}Phe$, in which the substituted amino acid is highly hydrophobic; although it gets closest to the exogenous oxygen atom of H_2O, it nevertheless has less effect on removing water when compared with $Glu^{374}His$ mutant where the substituted amino acid (at a greater

TABLE II

DdH Gibbs' energies (kcal/mol) of one, two, three, and four residue mutations for reaction step (3 → 4).

Residue substitutions for H_2O removal step	3 → 4
$Arg^{111}Glu$	−0.9
$Thr^{145}Val$	−1.3
$Ser^{177}Ala$	−0.1
$Glu^{240}His$	+1.1
$Glu^{374}His$	−3.1
$Tyr^{375}Phe$	−2.1
Combinations of	
$Glu^{374}His$ and $Tyr^{375}Phe$	−5.1
$Thr^{145}Val$, $Glu^{374}His$, and $Tyr^{375}Phe$	−6.2
$Arg^{111}Glu$, $Thr^{145}Val$, $Glu^{374}His$, and $Tyr^{375}Phe$	−7.5

distance from H_2O) is not only polar but also of opposite charge as well.

The negative partial charge on oxygen (−0.935) of H_2O repels the negatively charged carboxylate of Glu^{374} (q_{COO^-} = 0.547, −0.567, −0.563), thus making the water removal difficult. When Glu^{374} is replaced by a protonated histidine, the opposite effect is observed.

FRONTIER MOLECULAR ORBITAL ANALYSIS

Molecular orbital analysis is provided using frontier orbitals (HOMO, LUMO, and SOMO) in correlation with the formerly presented Gibbs' energies. Essentially, reduction for all three pathways are carried out on closed-shell clusters, that is, an e^- is transferred into the lowest unoccupied molecular orbital, H-cluster LUMO.

In the case of open-shell H-cluster protonation (both gas and aqueous enzyme Φ), a σ-bond is formed between a H^+ and (the exogenous ligand) OH^- by the interaction of electrons in the highest occupied molecular orbitals, viz., SOMO and HOMO. Conversely, when a H^+ is in close proxim-

TABLE IV

Interatomic distances between the oxygen (of exogenous H_2O; Fe_d-OH_2, compound 3) and the juxtaposed atoms of the residue R-groups.

Mutated DdH	H_2O oxygen	Å
$Arg^{111}Glu$ mutant		
O(ε)	$O(H_2O)$	17.507
O(ε)	$O(H_2O)$	18.259
$Thr^{145}Val$ mutant		
C(γ)	$O(H_2O)$	9.616
C(γ)	$O(H_2O)$	9.650
$Ser^{177}Ala$ mutant		
C(β)	$O(H_2O)$	6.077
$Glu^{240}His$ mutant		
N(δ)	$O(H_2O)$	12.395
N(ε)	$O(H_2O)$	11.666
$Glu^{374}His$ mutant		
N(δ)	$O(H_2O)$	9.631
N(ε)	$O(H_2O)$	9.038
$Tyr^{375}Phe$ mutant		
C(ζ)	$O(H_2O)$	7.724

TABLE III

Interatomic distances (Å) for wild-type and mutated DdH, between Fe_p and Fe_d, Fe_p and CO_b, Fe_d and CO_b, and Fe_d and H_2O, before and after H_2O removal (3 → 4).

Before H_2O removal	3 (Wild-type)	3 (Arg^{111} Glu mutant)	3 (Thr^{145} Val mutant)	3 (Glu^{374} His mutant)	3 (Tyr^{375} Phe mutant)
Fe_p-Fe_d	2.626	2.659	2.670	2.690	2.666
CO_b-Fe_p	1.959	1.963	1.968	1.975	1.991
CO_b-Fe_d	1.907	1.952	1.963	1.945	1.937
Fe_d-$O(H_2O)$	2.127	2.205	2.181	2.223	2.184
After H_2O removal	4 (Wild-type)	4 (Arg^{111}Glu mutant)	4 (Thr^{145} Val mutant)	4 (Glu^{374} His mutant)	4 (Tyr^{375} Phe mutant)
Fe_p-Fe_d	2.587	2.584	2.616	2.589	2.582
CO_b-Fe_p	1.939	2.006	2.003	2.008	2.005
CO_b-Fe_d	1.908	1.928	1.935	1.928	1.906

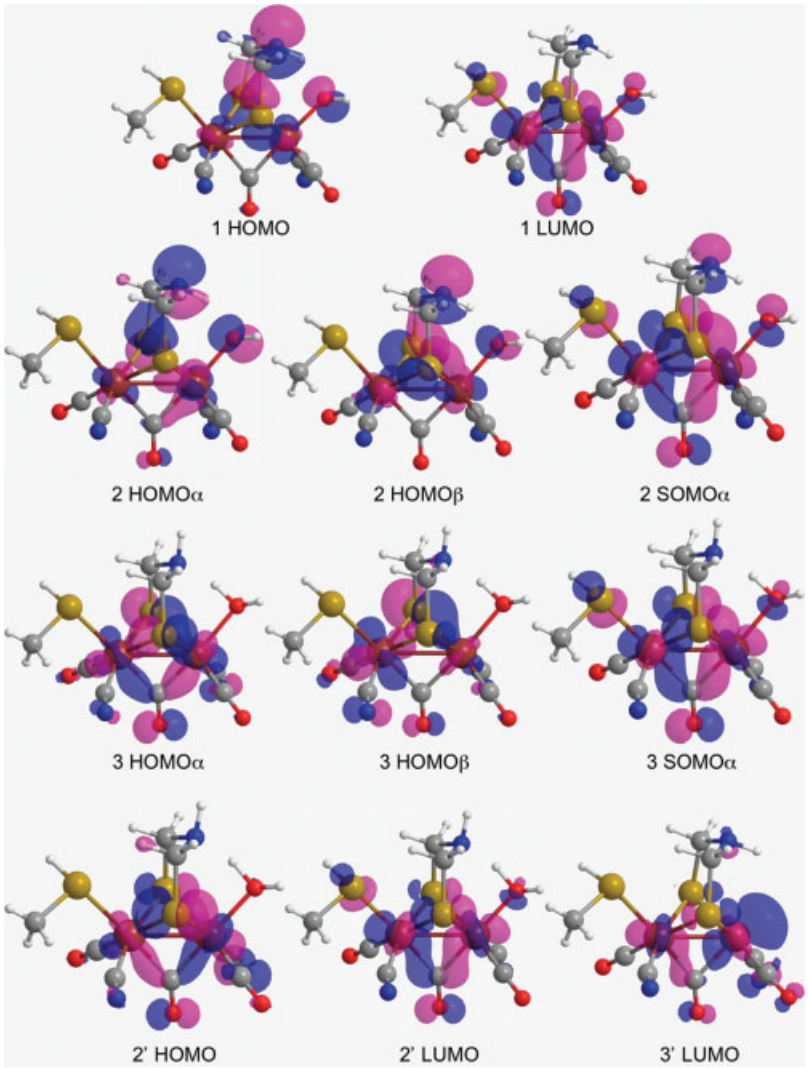

FIGURE 2. The frontier molecular orbitals from DFT calculations (B3LYP/6-31+G(d,p)). [Color figure can be viewed in the online issue, which is available at wileyonlinelibrary.com.]

ity to a closed-shell H-cluster, the resulting σ-bond is mainly due to the contribution of e^-s from HOMO and the H^+.

The [Fe-Fe]-hydrogenase H-cluster 1 of the wild-type enzyme becomes reduced (Scheme 1, 1 → 2), and according to the LUMO depiction (see Fig. 2), the transferred e^- appears to be localized in the vicinity of the di-iron atoms, Fe_p-Fe_d. However, according to the NBO partial charge results (see Fig. 3), the iron atoms (of hydrogenase H-cluster 1) do not have affinity for the approaching e^-, that is, q_{Fep} = −1.291 a.u. and q_{Fed} = −1.109 a.u. The fact that the reduction is endergonic ($\Delta G_{Enzyme\ \Phi}$ = +42.6 kcal/mol) corroborates the orbital analysis results, which indicate that e^- transfer to the cluster should be thermodynamically unfavorable due to existing negative charge on the di-iron atoms.

Regarding [Fe-Fe]-hydrogenase H-cluster 2, (2 → 3), the open shells, $SOMO_\alpha$, $HOMO_\alpha$, and $HOMO_\beta$, have similar orbital distribution over OH^- (Fig. 2), and could make a σ-bond with the incoming H^+; in conjunction with the NBO partial charge of the hydroxyl oxygen, q_O = −0.991 a.u., the large H^+ affinity for cluster 2, ΔG = −317.9 kcal/mol, (2 → 3) comes as no surprise.

In H-cluster 3, (3 → 4), the open shells, $HOMO_\alpha$, $HOMO_\beta$, and $SOMO_\alpha$, are diffused throughout the cluster except over the Fe_d-OH_2 bond, implying that the e^-s of the σ-bond, Fe_d-OH_2, reside in a lower energy state, which also explains the negative

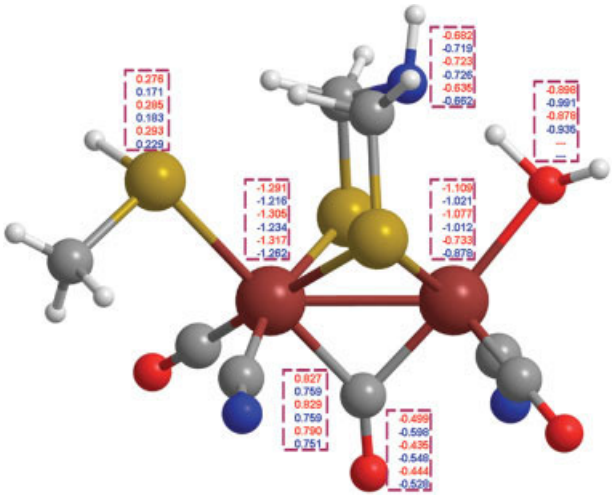

FIGURE 3. The NBO charges obtained from DFT calculations (B3LYP/6-31+G(d,p)). Charges are Given in a.u. for the following H-clusters: 1, 2, 2′, 3, 3′, and 4 starting from the top of the columns. [Color figure can be viewed in the online issue, which is available at wileyonlinel brary. com.]

NBO partial charges of both Fe_d ($q_{Fed} = -1.012$ a.u.), and the O ($q_O = -0.935$ a.u.) of H_2O. This fact may explain, therefore, the affinity of Fe_d for H_2O, that is, $\Delta G = +2.0$ kcal/mol.

For [Fe-Fe]-hydrogenase H-cluster 1, (Scheme 2, 1 → 2′), the HOMO is more diffused over Fe_d, DTMA bidentate ligand, and over the exogenous ligand, that is, OH^-. In spite of greater e^- orbital diffusion over the DTMA ligand, the H^+ becomes captured by OH^-, for it is a stronger base than the N of the DTMA bridge, as the NBO charges indicate ($q_O = -0.898$; $q_N = -0.682$). Note that these analyses also agree with the calculated hydrogenase H-cluster proton affinity, that is, $\Delta G = -236.8$ kcal/mol.

For H-cluster 2′, (Scheme 2, 2′ → 3′), HOMO is diffused over the center of Fe_p-Fe_d subcluster, CO_b, and over CN^- (Fe_d coordinated) which means that the e^-s of the σ-bond, Fe_d-OH_2, are situated in a lower energy state, explaining the negative NBO partial charges of both O (of H_2O, $q_O = -0.878$ a.u.) and Fe_d ($q_{Fed} = -1.077$ a.u.). This, then, accounts for the bond strength of Fe_d for H_2O, that is, $\Delta G = +22.9$ kcal/mol. In addition, from geometrical considerations, 2′ → 3′, it can be seen that CO_b-Fe_d bond becomes longer, viz., 1.932 → 1.942 Å [vs. 1.907 → 1.908 Å (in H-cluster 3, Scheme 1, 3 → 4)], which partially accounts for the more endergonic H_2O elimination process, coinciding with an increase of one order of magnitude for the Gibbs' energy difference (for water elimination in 2′ → 3′ vs. 3 → 4).

In H-cluster 3′, LUMO is mostly localized on the potential catalytic binding site. Upon the reduction of the H-cluster, (3′ → 4), the LUMO depiction shows that the e^- should become localized peripherally to the Fe_d. Then according to the NBO partial charges, that is, $q_{Fep} = -1.317$ a.u. and $q_{Fed} = -0.733$ a.u., in conjunction with the above presented LUMO depiction, the cluster reduction occurs with a rather high spontaneity, that is, $\Delta G_{Enzyme\ \Phi} = -59.4$ kcal/mol, although the di-iron atoms have rather high NBO charges.[9]

The LUMO on the wild-type hydrogenase H-cluster 2′ is delocalized on the two irons, Fe_p-Fe_d, DTMA sulfur atoms, and CO_b (Fig. 2). Cluster reduction (Scheme 3, 2′ → 3) occurs with a rather high spontaneity, that is, $\Delta G_{Enzyme\ \Phi} = -38.4$ kcal/mol, although the di-iron atoms have high NBO negative charges, that is, $q_{Fep} = -1.305$ a.u. and $q_{Fed} = -1.077$ a.u. [just as for H-cluster 3′, (3′ → 4)]. It ought to be noted that the e^- transfer occurs exergonically relative to the endergonic step (+42.6 kcal/mol) in Scheme 1, 1 → 2, perhaps because the total charge on each cluster is different, that is, cluster 2′ has charge 0 a.u., whereas 1 has a charge of −1 a.u.

Discussion

The comparison between gas phase and wild-type enzyme calculations, presented in this study, unambiguously shows that CO_b migration is key to enzyme inhibition by O_2. When CO_b is close to the Fe_d, DdH becomes reactivated, while, on the other hand, when CO_b is further away from Fe_d, wild-type enzyme H-cluster inactivation is observed. The displacement of CO_b is controlled by the apoenzyme, and can be further modulated by amino acid substitutions. In the wild-type enzyme, the protein environment impinges CO_b away from the catalytic site, Fe_d, leading to an exogenously inhibited hydrogenase, and thus hindering H_2O elimination. On the contrary, suitable residue substitutions can reverse the enzyme inhibition by al-

[9]Because NBO charges on iron atoms are both negatively charged, and the reaction proceeds exergonically, it means that the e^- is transferred due to a vicinal potential difference, with the e^- source most likely being the proximal cubane/cysteine (Fe_4S_4/Cys_4), cluster.

lowing CO_b to migrate towards Fe_d, concomitant with H_2O removal.

The potential reactivation pathway of Scheme 1 is rendered less promising by the protein environment due to step 1 → 2, which is rather endergonic.

Also, the reactivation pathway of [Fe-Fe]-hydrogenase H-cluster 4 (Scheme 2) cannot be realized because of the high nonspontaneous step for H_2O removal (2′ → 3′), $\Delta G_{\text{Enzyme }\Phi} = +22.9$ kcal/mol). As a result, this scheme does not seem to provide room for mutagenic enhancements (residue substitutions) that could improve H_2O removal.

However, in electrochemical settings, a hydrogenase can be adsorbed onto an electrode surface where the endergonic reductive step may be reversed by intramolecular changes (viz., apoenzyme amino acid substitutions) or extramolecular modifications (viz., voltage adjustment, or solution tuning such as pH modification, salt concentration changes, etc.).

The last reaction pathway of Scheme 3 provides the best chance for reactivating DdH because the only reaction step to overcome (H_2O removal) is barely endergonic ($\Delta G_{\text{Enzyme }\Phi} = +2.0$ kcal/mol), which can be accomplished by suitable amino acid substitutions.

DdH screening by residue deletions pointed out which residues may increase the removal of H_2O from the catalytic site. From residue deletion clues, single and multiple residue substitutions have led to exergonic H_2O removal (e.g., $Arg^{111}Glu$, $Thr^{145}Val$, $Glu^{374}His$, and $Tyr^{375}Phe$ providing $\Delta G = -7.5$ kcal/mol).

Conclusions

The DdH reactivation, according to pathway I, consists of an endergonic e^- transfer step (viz., $\Delta G_{\text{Enzyme }\Phi} = +42.6$ kcal/mol), followed by an exergonic H^+ transfer step (viz., $\Delta G_{\text{Enzyme }\Phi} = -317.9$ kcal/mol), and then an endergonic H_2O removal step (viz., $\Delta G_{\text{Enzyme }\Phi} = +2.0$ kcal/mol).

For reactivation pathway II, the [Fe-Fe]-hydrogenase H-cluster H^+ transfer occurs first ($\Delta G_{\text{Enzyme }\Phi} = -236.8$ kcal/mol), followed by H_2O removal ($\Delta G_{\text{Enzyme }\Phi} = +22.9$ kcal/mol), and then by e^- transfer ($\Delta G_{\text{Enzyme }\Phi} = -59.4$ kcal/mol), with all steps being exergonic, except for the removal of water.

Pathway III, however, proceeds by an exergonic protonation step (viz., $\Delta G_{\text{Enzyme }\Phi} = -236.8$ kcal/mol), an exergonic e^- transfer step (viz., $\Delta G_{\text{Enzyme }\Phi} = -38.4$ kcal/mol), followed by water removal step (viz., $\Delta G_{\text{Enzyme }\Phi} = +2.0$ kcal/mol), which is barely endergonic. Thus, the reason DdH intermediates of pathway III, rather than those of pathway I and II, were chosen to be residue mutated was to achieve a pathway that proceeds exergonically throughout. Results have been obtained for deleted, substituted, and combined (substitutions of) residues. Combinations of two, three, and four residues gave improved negative Gibbs' energies for the removal of water, relative to single substituted residues.

In pathway III, the endergonic step, for H_2O removal, was made to proceed more spontaneously by removing inhibitory residues, one at a time. The promising residues are ΔArg^{111}, ΔThr^{145}, ΔSer^{177}, ΔGlu^{240}, ΔGlu^{374}, and ΔTyr^{375}, and their respective Gibbs' energies are −0.7 kcal/mol, −0.2 kcal/mol, −0.5 kcal/mol, +0.8 kcal/mol, −1.6 kcal/mol, and +1.1 kcal/mol.

Individual residues were substituted, viz., $Arg^{111}Glu$, $Thr^{145}Val$, $Ser^{177}Ala$, $Glu^{240}His$, $Glu^{374}His$, and $Tyr^{375}Phe$. All substitutions resulted in improved spontaneity for H_2O removal, relative to residue deletions, except for $\Delta Ser^{177} \rightarrow Ser^{177}Ala$ ($\Delta G = -0.5$ kcal/mol → $\Delta G = -0.1$ kcal/mol), and $\Delta Glu^{240} \rightarrow Glu^{240}His$ ($\Delta G = +0.8$ kcal/mol → $\Delta G = +1.1$ kcal/mol).

From the successful, single residue substitutions, two, three, and four residue combinations were used to prepare DdH mutants for frequency calculations. The two residue combination, $Glu^{374}His$ and $Tyr^{375}Phe$, resulted in $\Delta G = -5.1$ kcal/mol; the three residue combination, $Thr^{145}Val$, $Glu^{374}His$, and $Tyr^{375}Phe$, provided a $\Delta G = -6.2$ kcal/mol, and the four residue combination, $Arg^{111}Glu$, $Thr^{145}Val$, $Glu^{374}His$, and $Tyr^{375}Phe$, gave a $\Delta G = -7.5$ kcal/mol. Although the H_2O removal thermodynamic trend is not precisely cumulative, it seems to point in that direction.

The wild-type DdH H-cluster bond distance, that is, Fe_d-CO_b, relative to that of the H-cluster (gas Φ), for H_2O elimination remains almost constant (viz., 1.907 Å → 1.908 Å), whereas the gas Φ^2 bond distance becomes smaller (viz., 1.945 Å → 1.850 Å), occurring with a concomitant exergonic H_2O removal; this, then, may partly explain why the removal of H_2O is exergonic for gas Φ, as opposed to the enzyme Φ.

Because pathway III has only the H_2O removal step to overcome to proceed exergonically, it was found to provide, to some extent, the sought after reactivation via residue substitutions. The step for H_2O removal from the wild-type hydrogenase

($\Delta G_{\text{Enzyme }\Phi}$ = +2.0 kcal/mol) shows that the distance between the Fe_d and CO_b remains approximately the same. However, the H_2O removal from the mutated enzyme proceeds exergonically, correlating to the movement of the CO_b towards the Fe_d. The following bond contractions, Fe_d-CO_b, have been obtained, viz., 0.024 Å for $Arg^{111}Glu$, 0.028 Å for $Thr^{145}Val$, 0.017 Å for $Glu^{374}His$, and 0.031 Å for $Tyr^{375}Phe$, corresponding to exergonic steps for water elimination. Additionally, bond contractions have been obtained between the iron atoms (ca. 0.1 Å), concurrent with H_2O dissociation.

We conclude by postulating that even a single and proper residue (experimental) substitution, like $\Delta Glu^{374} \rightarrow Glu^{374}His$ ($\Delta G = -1.6$ kcal/mol $\rightarrow \Delta G = -3.1$ kcal/mol), can reactivate the [Fe-Fe]-hydrogenase.

We presented here a complete mechanistic picture of the reactivation reaction of the H-cluster and the role of the bridging carbonyl in modulating this reactivation. We compared the gas phase results with enzyme calculations and show how careful residue mutations can have a significant effect on the electronic structure of H-cluster. We have identified for the first time amino acid residues surrounding the active site that can be used to modulate the reactivity of [Fe-Fe]-hydrogenase. Our calculations and the different analyses (i.e., thermodynamic, geometrical, and electronic) emphasize that all these structural data pertaining to different origins (electronic, geometric, thermodynamics) concur in the suggested picture for the reaction mechanism of the reactivation of wild-type [Fe-Fe]-hydrogenase.

ACKNOWLEDGMENTS

Computational resources have been provided by the National Center for Supercomputer Applications (University of Illinois) and the Ohio Supercomputer Center.

References

1. Dogaru, D.; Motiu, S.; Gogonea, V. Int J Quantum Chem 2009, 109, 876.
2. Motiu, S.; Dogaru, D.; Gogonea, V. Int J Quantum Chem 2007, 107, 1248.
3. Liu, Z.-P.; Hu, P. J Am Chem Soc 2002, 124, 5175.
4. Vignais, P. M.; Billoud, B.; Meyer J. FEMS Microbiol Rev 2001, 25, 455.
5. Adams, M. W. W.; Stiefel, E. I. Science 1998, 282, 1842.
6. Frey, M. Chembiochem 2002, 3, 153.
7. Liu, X.; Ibrahim, S. K.; Tard, C.; Pickett, C. J. Coord Chem Rev 2005, 15–16, 1641.
8. Adams, M. W. W. Biochim Biophys Acta 1990, 1020, 115.
9. Albracht, S. P. J. Biochim Biophys Acta 1994, 1118, 167.
10. Happe, R. P.; Roseboom, W.; Pierik, A. J.; Albracht, S. P.; Bagley, K. A. Nature 1997, 385, 126.
11. Melis, A.; Zhang, L.; Forestier, M.; Ghirardi, M. L.; Seibert, M. Plant Physiol 2000, 122, 127.
12. Peters, J. W.; Lanzilotta, W. N.; Lemon, B. J.; Seefeldt, L. C. Science 1998, 282, 1853.
13. Lemon, B. J.; Peters, J. W. Biochemistry 1998, 38, 12969.
14. Nicolet, Y.; Piras, C.; Legrand, P.; Hatchikian, E. C.; Fontecilla-Camps, J. C. Structure 1999, 7, 13.
15. Liu, Z.-P.; Hu, P. J Chem Phys 2002, 117, 8177.
16. Bruschi, M.; Fantucci, P.; De Gioia, L. Inorg Chem 2002, 41, 1421.
17. Bruschi, M.; Fantucci, P.; De Gioia, L. Inorg Chem 2003, 42, 4773.
18. Bruschi, M.; Fantucci, P.; De Gioia, L. Inorg Chem 2004, 43, 3733.
19. Cao, Z.; Hall, M. B. J Am Chem Soc 2001, 123, 3734.
20. Fan, H.-J.; Hall, M. B. J Am Chem Soc 2001, 123, 3828.
21. Greco, C.; Bruschi, M.; De Gioia, L.; Ryde, U. Inorg Chem 2007, 46, 5911.
22. Zampella, G.; Bruschi, M.; Fantucci, P.; Razavet, M.; Pickett, C. J.; De Gioia, L. Chem Eur J 2005, 11, 509.
23. Popescu, C. V.; Munck, E. J Am Chem Soc 1999, 121, 7877.
24. Tye, J. W.; Darensbourg, M. Y.; Hall, M. B. J Comput Chem 2006, 27, 1454.
25. Darensbourg, M. Y. Nature 2005, 433, 589.
26. Madamwar, D.; Garg, N.; Shah, V. World J Microbiol Biotechnol 2000, 16, 757.
27. He, C. J.; Wang, M.; Li, M. A.; Sun, L. C. Prog Chem 2004, 16, 250.
28. Chang, C. H.; King, P. W.; Ghirardi, M. L.; Kim, K. Biophys J 2007, 93, 3034.
29. Long, H.; Chang, C. H.; King, P. W.; Ghirardi, M. L.; Kim, K. Biophys J 2008, 95, 3753.
30. Rappe, A. K.; Goddard, W. A. J Phys Chem 1991, 95, 3358.
31. Zilberman, S.; Stiefel, E. I.; Cohen, M. H.; Car, R. Inorg Chem 2006, 45, 5715.
32. Silaghi-Dumitrescu, I.; Bitterwolf, T. E.; King, R. B. J Am Chem Soc 2006, 128, 5342.
33. Boyke, C. A.; Rauchfuss, T. B.; Wilson, S. R.; Rohmer, M.-M.; Benard, M. J Am Chem Soc 2004, 126, 15151.
34. Adams, M. W. W.; Mortenson, L. E. J Biol Chem 1984, 259, 7045.
35. Rusnak, F. M.; Adams, M. W. W.; Mortenson, L. E.; Munck, E. J Biol Chem 1987, 262, 38.
36. Adams, M. W. W. J Biol Chem 1987, 262, 15054.
37. Trohalaki, S.; Pachter, R. Energy fuels 2007, 21, 2278.
38. Greco, C.; Bruschi, M.; Heimdal, J.; Fantucci, P.; De Gioia, L.; Ryde, U., Inorg Chem 2007, 46, 7256.
39. Greco, C.; Bruschi, M.; Fantucci, P.; De Gioia, L. Eur J Inorg Chem 2007, 13, 1835.

40. Greco, C.; Zampella, G.; Bertini, L.; Bruschi, M.; Fantucci, P.; De Gioia, L. Inorg Chem 2007, 46, 108.
41. Bruschi, M.; Zampella, G.; Fantucci, P.; De Gioia, L., Coord Chem Rev 2005, 15–16, 1620.
42. Armstrong, F. A. Curr Opin Chem Biol 2004, 8, 133.
43. Rauchfuss, T. B. Inorg Chem 2004, 43, 14–26.
44. Evans, D. J.; Pickett, C. J. Chem Soc Rev 2003, 35, 268.
45. Chen, Z.; Lemon, B. J.; Huang, S.; Swartz, D. J.; Peters, J. W.; Bagley, K. A. Biochemistry 2002, 41, 2036.
46. Horner, D. S.; Heil, B.; Happe, T.; Embley, T. M. Trends Biochem Sci 2002, 27, 148.
47. Nicolet, Y.; Cavazza, C.; Fontecilla-Camps, J. C. J Inorg Biochem 2002, 91, 1.
48. Lyon, E. J.; Georgakaki, I. P.; Reibenspies, J. H.; Darensbourg, M. Y. Angew Chem Int Ed Engl 1999, 38, 3178.
49. Cloirec, A. L.; Best, S. P.; Borg, S.; Davies, S. C.; Evans, D. J.; Hughes, D. L.; Pickett, C. J. Chem Commun 1999, 22, 2285.
50. Rauchfuss, T. B.; Contakes, S. M.; Schmidt, M. J Am Chem Soc 1999, 121, 9736.
51. Lai, C.-H.; Lee, W.-Z.; Miller, M. L.; Reibenspies, J. H.; Darensbourg, D. J.; Darensbourg, M. Y. J Am Chem Soc 1998, 120, 10103.
52. Zambrano, I. C.; Kowal, A. T.; Mortenson, L. E.; Adams, M. W. W.; Johnson, M. K. J Biol Chem 1989, 264, 20974.
53. Pierik, A. J.; Hagen, W. R.; Redeker, J. S.; Wolbert, R. B. G.; Boersma, M.; Verhagen, M. F.; Grande, H. J.; Veeger, C.; Mustsaers, P. H. A.; Sand, R. H.; Dunham, W. R. Eur J Biochem 1992, 209, 63.
54. De Lacey, A. L.; Stadler, C.; Cavazza, C.; Hatchikian, E. C.; Fernandez, V. M. J Am Chem Soc 2000, 122, 11232.
55. Nicolet, Y.; De Lacey, A. L.; Vernede, X.; Fernandez, V. M.; Hatchikian, E. C.; Fontecilla-Camps, J. C. J Am Chem Soc 2001, 123, 1596.
56. Dapprich, S.; Komaromi, I.; Byun, K. S.; Morokuma, K.; Frisch, M. J. J Mol Struct (Theochem) 1999, 461, 1.
57. Rappe, A. K.; Casewit, C. J.; Colwell, K. S.; Goddard III, W. A.; Skiff, W. M. J Am Chem Soc 1992, 114, 10024.
58. Frisch, M. J.; Trucks, G. W.; Schlegel, H. B.; Scuseria, G. E.; Robb, M. A.; Cheeseman, J. R.; Montgomery, J. J. A.; Vreven, T.; Kudin, K. N.; Burant, J. C.; Millam, J. M.; Iyengar, S. S.; Tomasi, J.; Barone, V.; Mennucci, B.; Cossi, M.; Scalmani, G.; Rega, N.; Petersson, G. A.; Nakatsuji, H.; Hada, M.; Ehara, M.; Toyota, K.; Fukuda, R.; Hasegawa, J.; Ishida, M.; Nakajima, T.; Honda, Y.; Kitao, O.; Nakai, H.; Klene, M. L. X.; Knox, J. E.; Hratchian, H. P.; Cross, J. B.; Bakken, V.; Adamo, C.; Jaramillo, J.; Gomperts, R.; Stratmann, R. E.; Yazyev, O.; Austin, A. J.; Cammi, R.; Pomelli, C.; Ochterski, J. W.; Ayala, P. Y.; Morokuma, K.; Voth, G. A.; Salvador, P.; Dannenberg, J. J.; Zakrzewski, V. G.; Dapprich, S. D. A. D.; Strain, M. C.; Farkas, O.; Malick, D. K.; Rabuck, A. D.; Raghavachari, K.; Foresman, J. B.; Ortiz, J. V.; Cui, Q.; Baboul, A. G.; Clifford, S.; Cioslowski, J.; Stefanov, B. B.; Liu, G.; Liashenko, A.; Piskorz, P.; Komaromi, I.; Martin, R. L.; Fox, D. J.; Keith, T.; Al-Laham, M. A.; Peng, C. Y.; Nanayakkara, A.; Challacombe, M.; Gill, P. M. W.; Johnson, B.; Chen, W.; Wong, M. W.; Gonzalez, C.; Pople, J. A. Gaussian 03, Revision C. 02; Gaussian, Inc.: Wallingford CT, 2004.
59. Becke, A. D. J Chem Phys 1993, 98, 5648.
60. Lee, C.; Yang, W.; Parr, R. G. Phys Rev B 1988, 37, 785.
61. Berendsen, H. J. C.; van der Spoel, D. Comp Phys Comm 1995, 91, 43.
62. Lindahl, E.; Hess, B. J Mol Mod 2001, 7, 306.
63. DeLano, W. L. The PyMOL Molecular Graphics System 2002; DeLano Scientific: Palo Alto, CA, USA, 2002.
64. Guex, N.; Peitsch, M. C. Electrophoresis 1997, 18, 2714.